Improvement of reliability in multi-interferometer-based counterfactual deterministic communication with dissipation compensation

CHAO LIU,[1] JINHONG LIU,[1] JUNXIANG ZHANG,[1,2,*] AND SHIYAO ZHU[1,2,3]

[1]*State Key Laboratory of Quantum Optics and Quantum Optics Devices, Institute of Opto-electronics, Shanxi University, Taiyuan, 030006, China*
[2]*Department of Physics, Zhejiang University, Hangzhou, 310027, China*
[3]*Beijing Computational Science Research Center, Beijing, 100084, China*
junxiang_zhang@zju.edu.cn

Abstract: The direct counterfactual quantum communication (DCQC) is a surprising phenomenon that quantum information can be transmitted without using any carriers of physical particles. The nested interferometers are promising devices for realizing DCQC as long as the number of interferometers goes to be infinity. Considering the inevitable loss or dissipation in practical experimental interferometers, we analyze the dependence of reliability on the number of interferometers, and show that the reliability of direct communication is being rapidly degraded with the large number of interferometers. Furthermore, we simulate and test this counterfactual deterministic communication protocol with a finite number of interferometers, and demonstrate the improvement of the reliability using dissipation compensation in interferometers.

OCIS codes: (270.0270) Quantum optics; (270.5565) Quantum communications; (270.5585) Quantum information and processing.

References and links

1. C. H. Bennett and G. Brassard, in *Proceedings of the IEEE international conference on computers, systems and signal processing, Bangalore, India* (IEEE, 1984), p. 175.
2. C. H. Bennett, G. Brassard, and N. D. Mermin, "Quantum cryptography without bell's theorem," Phys. Rev. Lett. **68**(5), 557–559 (1992).
3. G. C. Guo and B. S. Shi, "Quantum cryptography based on interaction-free measurement," Phys. Lett. A **256**(2-3), 109–112 (1999).
4. H. K. Lo and H. F. Chau, "Unconditional security of quantum key distribution over arbitrarily long distances," Science **283**(5410), 2050–2056 (1999).
5. W. Y. Hwang, D. Ahn, and S. W. Hwang, "Quantum gambling using two nonorthogonal states," Phys. Rev. A **64**(6), 064302 (2001).
6. L. Xiao, C. Wang, W. Zhang, Y. D. Huang, J. D. Peng, and G. L. Long, "Efficient strategy for sharing entanglement via noisy channels with doubly entangled photon pairs," Phys. Rev. A **77**(4), 042315 (2008).
7. G. L. Long and X. S. Liu, "Theoretically efficient high-capacity quantum-key-distribution scheme," Phys. Rev. A **65**(3), 032302 (2002).
8. A. K. Ekert, "Quantum cryptography based on Bell's theorem," Phys. Rev. Lett. **67**(6), 661–663 (1991).
9. C. H. Bennett, "Quantum cryptography using any two nonorthogonal states," Phys. Rev. Lett. **68**(21), 3121–3124 (1992).
10. C. Silberhorn, N. Korolkova, and G. Leuchs, "Quantum key distribution with bright entangled beams," Phys. Rev. Lett. **88**(16), 167902 (2002).
11. R. García-Patrón and N. J. Cerf, "Continuous-variable quantum key distribution protocols over noisy channels," Phys. Rev. Lett. **102**(13), 130501 (2009).
12. N. J. Cerf, M. Lévy, and G. V. Assche, "Quantum distribution of Gaussian keys using squeezed states," Phys. Rev. A **63**(5), 052311 (2001).
13. V. Scarani, A. Acín, G. Ribordy, and N. Gisin, "Quantum cryptography protocols robust against photon number splitting attacks for weak laser pulse implementations," Phys. Rev. Lett. **92**(5), 057901 (2004).
14. X. B. Wang, L. Yang, C. Z. Peng, and J. W. Pan, "Decoy-state quantum key distribution with both source errors and statistical fluctuations," New J. Phys. **11**(7), 075006 (2009).

15. X. B. Wang, "Beating the photon-number-splitting attack in practical quantum cryptography," Phys. Rev. Lett. **94**(23), 230503 (2005).
16. B. Huttner, N. Imoto, N. Gisin, and T. Mor, "Quantum cryptography with coherent states," Phys. Rev. A **51**(3), 1863–1869 (1995).
17. S. K. Liao, W. Q. Cai, W. Y. Liu, L. Zhang, Y. Li, J. G. Ren, J. Yin, Q. Shen, Y. Cao, Z. P. Li, F. Z. Li, X. W. Chen, L. H. Sun, J. J. Jia, J. C. Wu, X. J. Jiang, J. F. Wang, Y. M. Huang, Q. Wang, Y. L. Zhou, L. Deng, T. Xi, L. Ma, T. Hu, Q. Zhang, Y. A. Chen, N. L. Liu, X. B. Wang, Z. C. Zhu, C. Y. Lu, R. Shu, C. Z. Peng, J. Y. Wang, and J. W. Pan, "Satellite-to-ground quantum key distribution," Nature **549**(7670), 43–47 (2017).
18. L. M. Duan, M. D. Lukin, J. I. Cirac, and P. Zoller, "Long-distance quantum communication with atomic ensembles and linear optics," Nature **414**(6862), 413–418 (2001).
19. F. G. Deng and G. L. Long, "Secure direct communication with a quantum one-time pad," Phys. Rev. A **69**(5), 052319 (2004).
20. F. G. Deng, G. L. Long, and X. S. Liu, "Two-step quantum direct communication protocol using the Einstein-Podolsky-Rosen pair block," Phys. Rev. A **68**(4), 042317 (2003).
21. J. Y. Hu, B. Yu, M. Y. Jing, L. T. Xiao, S. T. Jia, G. Q. Qin, and G. L. Long, "Experimental quantum secure direct communication with single photons," Light Sci. Appl. **5**(9), e16144 (2016).
22. W. Zhang, D. S. Ding, Y. B. Sheng, L. Zhou, B. S. Shi, and G. C. Guo, "Quantum secure direct communication with quantum memory," Phys. Rev. Lett. **118**(22), 220501 (2017).
23. F. Zhu, W. Zhang, Y. B. Sheng, and Y. D. Huang, "Experimental long-distance quantum secure direct communication," Science Bulletin **62**(22), 1519–1524 (2017).
24. A. C. Elitzur and L. Vaidman, "Quantum mechanical interaction-free measurements," Found. Phys. **23**(7), 987–997 (1993).
25. T. G. Noh, "Counterfactual quantum cryptography," Phys. Rev. Lett. **103**(23), 230501 (2009).
26. G. Brida, A. Cavanna, I. P. Degiovanni, M. Genovese, and P. Traina, "Experimental realization of counterfactual quantum cryptography," Laser Phys. Lett. **9**(3), 247–252 (2012).
27. Y. Liu, L. Ju, X. L. Liang, S. B. Tang, G. L. Tu, L. Zhou, C. Z. Peng, K. Chen, T. Y. Chen, Z. B. Chen, and J. W. Pan, "Experimental demonstration of counterfactual quantum communication," Phys. Rev. Lett. **109**(3), 030501 (2012).
28. Z. Q. Yin, H. W. Li, W. Chen, Z. F. Han, and G. C. Guo, "Security of counterfactual quantum cryptography," Phys. Rev. A **82**(4), 042335 (2010).
29. P. G. Kwiat, A. G. White, J. R. Mitchell, O. Nairz, G. Weihs, H. Weinfurter, and A. Zeilinger, "High-efficiency quantum interrogation measurements via the quantum zeno effect," Phys. Rev. Lett. **83**(23), 4725–4728 (1999).
30. B. Misra and E. C. G. Sudarshan, "The Zeno's paradox in quantum theory," Phys. **18**(4), 756–763 (1977).
31. A. Peres, "Zeno paradox in quantum theory," Am. J. Phys. **48**(11), 931–932 (1980).
32. G. S. Agarwal and S. P. Tewari, "An all-optical realization of the quantum Zeno effect," Phys. Lett. A **185**(2), 139–142 (1994).
33. H. Salih, Z.-H. Li, M. Al-Amri, and M. S. Zubairy, "Protocol for direct counterfactual quantum communication," Phys. Rev. Lett. **110**(17), 170502 (2013).
34. Y. Cao, Y. H. Li, Z. Cao, J. Yin, Y. A. Chen, H. L. Yin, T. Y. Chen, X. Ma, C. Z. Peng, and J. W. Pan, "Direct counterfactual communication via quantum Zeno effect," Proc. Natl. Acad. Sci. U.S.A. **114**(19), 4920–4924 (2017).
35. J. Peise, B. Lücke, L. Pezzè, F. Deuretzbacher, W. Ertmer, J. Arlt, A. Smerzi, L. Santos, and C. Klempt, "Interaction-free measurements by quantum Zeno stabilization of ultracold atoms," Nat. Commun. **6**, 6811 (2015).
36. C. Liu, J. Liu, J. Zhang, and S. Zhu, "The experimental demonstration of high efficiency interaction-free measurement for quantum counterfactual-like communication," Sci. Rep. **7**(1), 10875 (2017).
37. A. Danan, D. Farfurnik, S. Bar-Ad, and L. Vaidman, "Asking photons where they have been," Phys. Rev. Lett. **111**(24), 240402 (2013).

1. Introduction

Quantum communication has attracted more and more attentions due to its potential for providing absolute secret communications and high speed data processing. It uses quantum principles to encoding information in quantum states, usually know as photons, ensuring the information be transmitted in an absolutely secure way. As a kind of quantum communication for deterministic secure communication, the quantum key distribution (QKD) protocol of BB84 was firstly proposed, it used single-photon polarization states to transmit the information and was provably secure, any attempt to intercept the information is likely to destroy the photon, and be found immediately [1]. And subsequently, a series of theoretical and experimental investigations were carried out on single-photon-based quantum information processing and secure communication [2–7]. The other QKD schemes were also investigated based on entangled photons, bright entangled beams and squeezed states [8–12].

For more practical uses, the QKD protocol of SARG04 [13] and decoy state method [14] were presented with weak pulses, it needs the quantum key for preventing the photon number splitting (PNS) attack [15, 16] because of the probability of existing two or more photons in weak pulse. Very recently, the satellite-ground QKD with decoy-state method was investigated [17]. These prominent quantum communication systems have the common feature of employing actual physical signal for information transfer. Physical transportation of quantum information may not a viable solution for long-distance quantum communication [18] because the interaction of the quantum system with its environment changes the state of system, and also the transporting single photons may be lost while passing through the transmission channel, leading to the reduction of efficiency. Quantum secure direct communication (QSDC) protocol was therefore presented to avoid eavesdrop via communicating messages directly without encryption and decryption processes [19, 20], and experimentally demonstrated with single photons, entangled EPR pairs and quantum memory [21–23].

Based on the idea of interaction-free measurement (IFM) [24], the counterfactual QKDs were represented [25–27], it means that the distribution of a quantum key could be achieved even when the encoded particle did not traverse through the quantum channel. The security of this kind of counterfactual quantum communication (CQC) was analyzed [28], and the experimental demonstration of CQC was accomplished as a direct verification and testing of this protocol [27]. Furthermore, based on IFM and quantum Zeno effect [29–32], the direct counterfactual quantum communication (DCQC) in a nested Mach-Zehnder interferometers (MZIs) was proposed [33], and the feasibility was confirmed by the experimental study [34]. Very recently, the experiment in cold atoms showed the potential application of IFM and quantum Zeno effect for possible CQC in atom optics [35].

In order to achieve a full DCQC in the nested interferometer scheme [33], the number of interferometers is needed to be a value of infinity in the ideal limit, and the scheme is confined to a necessary condition that all operational processes are in the ideal case. However, for a practical interferometer device, the effect of the loss and dissipation caused by the optical components and transporting channels will lead to the degraded performance on system running.

In this paper, we give the theoretical discussion about the effects of the loss or dissipation on the reliability and efficiency of the interferometer-based DCQC scheme, and present the optimum number selection of the interferometers for DCQC when the losses or dissipations are taken into account. We therefore present an experimental investigation of the reliability of direction communication in nested MZIs with finite M and N beam splitters, demonstrating the improvement of reliability using dissipation compensation. For the DCQC protocol, there is no overlap of the forward and the backward evolving wave functions when Bob blocks the transmission channel, as a result, Eve can get the message without being detected by performing weak measurement of the projection on the transmission channel. So that the protocol we simulated is a counterfactual deterministic communication scheme without the capability to detect eavesdropping.

2. The interferometer-based direct communication scheme

The nested MZIs are sketched in Fig. 1. M-1 big MZIs are connected in series, in which there are N-1 small MZIs connected in series. M and N are the number of the beam splitters (BSs) of the big MZIs and small MZIs. The beam splitters (blue rectangles) of BS_M (in big MZIs) and BS_N (in small MZIs) are specially designed with the reflectivity $R_M = \cos^2(\pi/2M)$ and $R_N = \cos^2(\pi/2N)$ for special consideration of interaction-free effect, which means that the information in the transmission channel can be detected without any interaction. The HR_M and HR_N, shown in dark rectangles, are high reflection mirrors. The piezoelectric transducers (PZTs) on the mirrors of HR_M and HR_N are used to lock the phase difference of each of MZIs. The detectors D_1, D_2 and D_3 are used to measure the output signals of the MZIs. The input state

represented by the annihilation operator $\hat{a}_{in}$, which is on the side of Alice, is incident into the first BS_M while vacuum field represented by $\hat{a}_v$ is introduced at the other end of the first BS_M. The blocks indicated by brown triangles can be turned on (logic 0) and off (logic 1), and are controlled by the Bob. Bob make the choice of logic 0 or 1, resulting in the input light to be detected at D_1 or D_2 due to the interferences of different MZIs. Therefore, based on high efficiency interaction-free measurement with quantum Zeno effect [36], the information communication can be completed under the operation of Alice and Bob with a stream of photons (or a coherent light [37]).

The quality of this communication system can be described by the reliability η_0 (the probability ratio $P(D_1)/P(D_2)$) and η_1 (the probability ratio $P(D_2)/P(D_1)$) for the case of logic 0 and logic 1, respectively. $P(D_{1,2})$ is the probability of detecting the input photons or light at D_1 or D_2. Correspondingly, the higher the values of η_0 and η_1 are, the more reliable or efficient the communication system is.
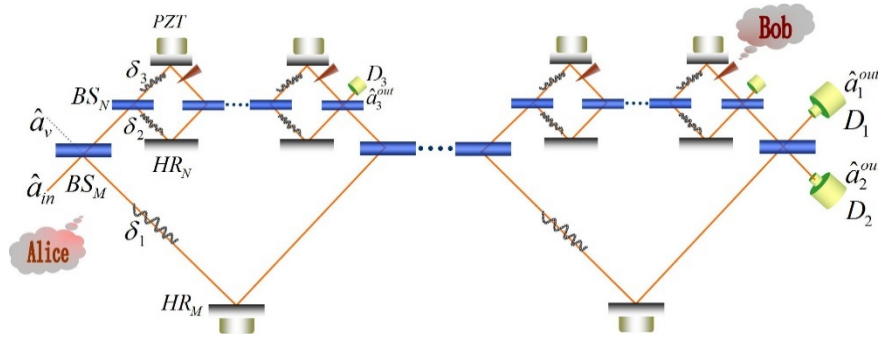

Fig. 1. Schematic diagram of the nested interferometers for direct communication.

3. The consideration of loss or dissipation in nested interferometers

In this complex experimental interferometer scheme, as shown in Fig. 1, the losses or dissipations in each path of interferometers are inevitable. Here you can simplify the paths as mail three parts: the path in the big MZIs below the BS_M, the path in the small MZIs between the BS_M and BS_N, and the path in the small MZIs above the BS_N. The losses or dissipations in these three paths are presented by δ_1, δ_2 and δ_3 respectively. Then we use the transfer-matrix method to describe the dissipation effect of the input state while passing through the big or small MZI, given by

$$\Gamma_M = \begin{pmatrix} \sqrt{1-\delta_1} & 0 \\ 0 & \sqrt{1-\delta_2}^N \end{pmatrix}, \Gamma_N = \begin{pmatrix} \sqrt{1-\delta_2} & 0 \\ 0 & \sqrt{1-\delta_3}^N \end{pmatrix}.$$

$$(1)$$

The effect of the phase shift in one path of each big MZI or small MZI is represented as

$$W_M = \begin{pmatrix} e^{i\varphi} & 0 \\ 0 & 1 \end{pmatrix}, W_N = \begin{pmatrix} 1 & 0 \\ 0 & e^{i\varphi} \end{pmatrix},$$

$$(2)$$

where φ or ϕ is the phase difference of each big MZI or small MZI. The two kinds of beam splitters (BS_M, BS_N) are expressed as

$$T_{BS_M} = \begin{pmatrix} r_m & -t_m \\ t_m & r_m \end{pmatrix}, T_{BS_N} \begin{pmatrix} r_n & -t_n \\ t_n & r_n \end{pmatrix},$$

(3)

where $r_m = \cos(\pi/2M)$ and $r_n = \cos(\pi/2N)$ are the reflection amplitudes of the BS_M and BS_N respectively. Meanwhile, $t_m = \sin(\pi/2M)$ and $t_n = \sin(\pi/2N)$ are the transmission amplitudes of the BS_M and BS_N respectively.

According to the matrix transformation relation $(\hat{a}_2^{out}, \hat{a}_1^{out})^T = T^{w(1,0)}(\hat{a}_{in}, \hat{a}_v)$ between the input state (represented by the column vector $(\hat{a}_{in}, \hat{a}_v)^T$) and the output state $(\hat{a}_2^{out}, \hat{a}_1^{out})^T$, we can obtain the output probability at detectors of D_1 and D_2. The values of $P(D_1)$ and $P(D_2)$ are proportional to the square of the matrix elements $T_{21}^{w(1,0)}$ and $T_{11}^{w(1,0)}$, $T^{w(1,0)}$ is the transformation matrix for the case of logic 0 or logic 1.
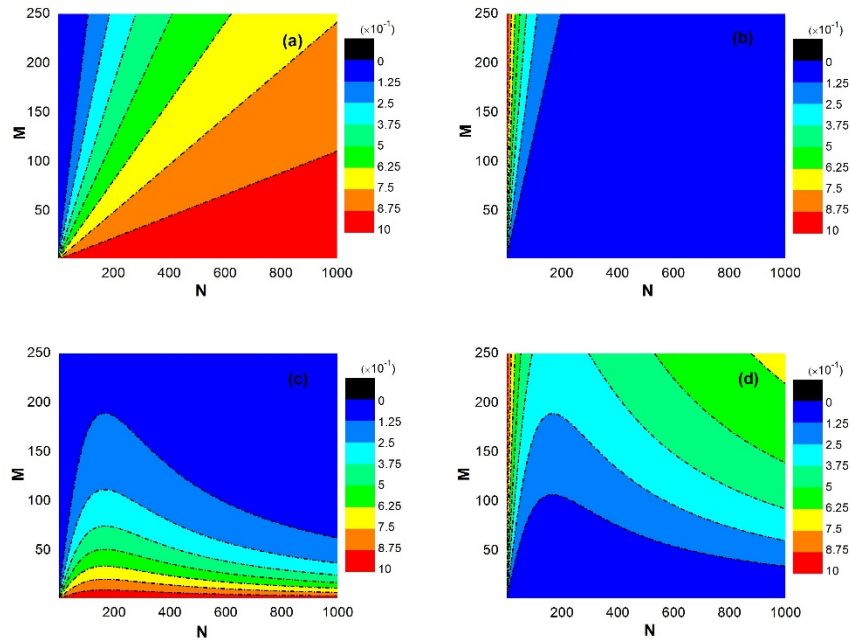

Fig. 2. The output probability without loss or dissipation: (a) $P(D_1)$ at D_1. (b) $P(D_2)$ at D_2; The output probability with loss or dissipation: (c) $P(D_1)$ at D1. (d) $P(D_2)$ at D_2.

For the case of logic 0 with blocks tuning on, the system consists M-1 big interferometers in the chained structure. As a result, the transfer matrix of the system can be represented as

$$T^{w(0)} = (T_{BS_M} \cdot T_M \cdot W_M \cdot \Gamma_M)^{M-1} \cdot T_{BS_M},$$

(4)

Where the transfer matrix T_M represents the effect of reflection of N BS_N between two adjacent BS_Ms, which is given by

$$T_M \begin{pmatrix} 1 & 0 \\ 0 & \cos^N \dfrac{\pi}{2N} \end{pmatrix}.$$

(5)

On the other hand, for the case of logic 1 with blocks tuning off, the system consists not only the *M*-1 big interferometers but also the *N*-1 small interferometers in the chained and nested structure, leading to the total transfer matrix in the form

$$T^{w(1)} = (T_{BS_M} \cdot W_M \cdot \Gamma_D)^{M-1} \cdot T_{BS_M}. \tag{6}$$

According to the effect of outputs in the small MZIs after (*N*-1)th loop, the matrix Γ_D could be written as

$$\Gamma_D = \begin{pmatrix} \sqrt{1-\delta_1} & 0 \\ 0 & T_{11}^{inn} \end{pmatrix}, \tag{7}$$

where T_{11}^{inn} is the matrix element of the inner transfer matrix for *N*-1 small MZIs, which can be calculated from the formula

$$T^{inn} = (T_{BS_N} \cdot W_N \cdot \Gamma_N)^{N-1} \cdot T_{BS_N}. \tag{8}$$

In Fig. 2, we plot the output probability at D_1 and D_2 for logic 0 when the phase of the interferometers is $\varphi = 0$. Figure 2(a) and 2(b) are the results for the ideal case without loss or dissipation, and Fig. 2(c) and 2(d) show the results when considering the loss or dissipation with the value of $\delta_1 = 10^{-4}, \delta_2 = 0.9\delta_1, \delta_3 = 0.9\delta_2$. For the case of logic 0, the output light of the chained interferometer is obtained at D_1, while D_2 detects few light, as seen from Fig. 2(a). It is also shown that the output probability at D_1 increases with the increase of *N* and *M*, and it approaches to 1 when *N* and *M* are larger enough. However, once the losses or dissipations are introduced in the interferometers, the output probability at D_1 will decreases with the increase of *N* and *M*, especially with large *M*. Increasing *M* means the increasing the number of big interferometers (*M*-1), and then the loss or dissipation will accumulate, leading to the decrease of detecting probability due to the worse of interference visibility.
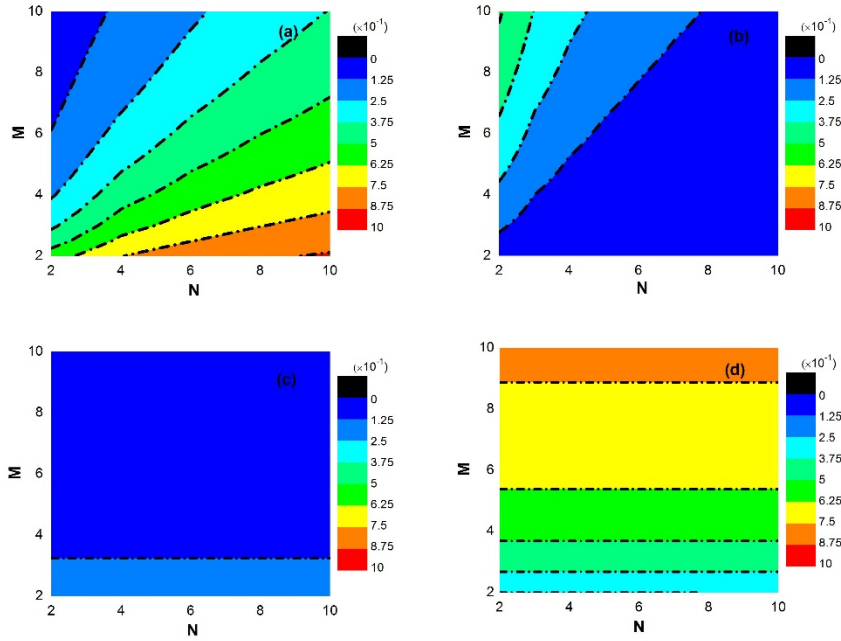
Fig. 3. The output probability with loss or dissipation for finite M and N. (a) and (b) $P(D_1)$ at D_1 and $P(D_2)$ at D_2 for logic 0; (c) and (d) $P(D_1)$ at D_1 and $P(D_2)$ at D_2 for logic 1.

Therefore, in practical interferometer-based direct communication scheme, we should make a choice of the finite numbers of M and N, as shown in Fig. 3 for $M, N \leq 10$. It is shown that the relative high probability at D_1 and a low probability at D_2 for the case of logic 0 are obtained (seen in Fig. 3(a) and 3(b)), and meanwhile, the relative low probability at D_1 and a high probability at D_2 for the case of logic 1 are also achieved (seen in Fig. 3(c) and 3(d)), e.g. $P(D_1)$ = 74.6% and $P(D_2)$ = 1.4% for logic 0, while $P(D_1)$ = 14.1% and $P(D_2)$ = 42.2% for logic 1 when $M = 3$, $N = 8$, it shows that the most part of light detected at D_1 or D_2 in Alice side corresponds to the Bob's choice for logic 0 or 1, i.e. the communication could be established between Alice and Bob. To note that the blocks for building of logic 0 and 1 are placed in transmission channel, which is up the BS_M and in the path of N small MZIs. Due to the small reflection of BS_M ($R_N = \cos^2(\pi/2N)$ with $N = 8$) and the phase locking of small MZIs with $\phi = 0$, very few portion of input light goes through the transmission channel path, and once a few light travels into the path in transmission channel, it will go out and be detected by D_3 due to the instructive interference of MZIs, ensuring that no light be found in the transmission channel in the next small chained MZIs.

Accordingly, we show the dependence of reliability $\eta_0 = P(D_1)/P(D_2)$ (for logic 0) and $\eta_1 = P(D_2)/P(D_1)$ (for logic 1) on the dissipation. Comparing the reliability for two cases of logic 0 and 1, η_0 (red line) is more sensitive to the dissipation as shown in Fig. 4(a), it decreases as the loss or dissipation increases. It should be noted that the reliability η_1 (black line) show slightly changes with the varies of dissipation, as seen in Fig. 4(b), proving indirectly that almost no light be transmitted in the transmission channel in small MZIs, and therefore any dissipation in MZIs do not affect the interference results in small MZIs, as a result, the reliability of η_1 shows less influence of the dissipation.
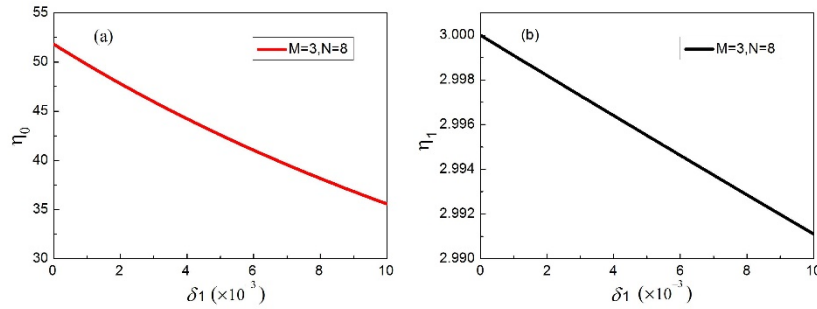
Fig. 4. The reliability as function of the dissipation $\delta_1(\delta_2 = 0.9\delta_1, \delta_3 = 0.9\delta_2)$ for (a) logic 0 and (b) logic 1 with $M = 3$, $N = 8$.

4. Optimization of experimental system by compensatory dissipation

According to the numerical analysis above, we found that the inevitable loss or dissipation gives rise to the reduction of the reliability of communication, and it also limits the use of large number of interferometers (or beam splitters in MZIs) in the practical experiment. Therefore we design the experiment with $M = 3$ and $N = 8$, as shown in Fig. 5, and specially in this scheme, we use the dissipation compensatory optics in the bottom path of the big MZIs to improve the reliability.
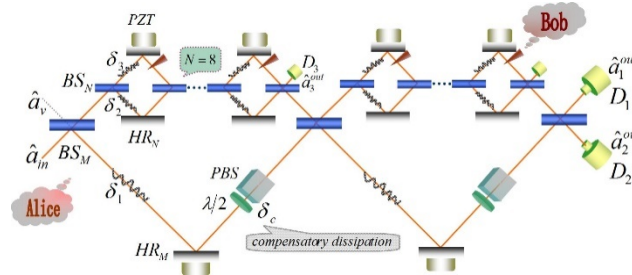

Fig. 5. The optimized experimental system of the direct communication

The compensation optical elements including half-wave plate ($\lambda / 2$) and polarization beam splitter (PBS) in one arm of big MZIs can be controlled continuously, as illustrated in Fig. 5. A weak horizontal polarization coherent light with the wavelength of 852 nm is used as the input light. Considering the compensatory dissipation, the whole transformation matrix can be expressed as

$$T_C^{w(0)} = (T_{BS_M} \cdot T_M \cdot W_M \cdot \Gamma_C)^{M-1} \cdot T_{BS_M}, \tag{9}$$

where Γ_C represents the compensatory dissipation effect of inner free-space between two adjacent BS$_M$s, which can be expressed as

$$\Gamma_C = \begin{pmatrix} \sqrt{1-(\delta_1 + \delta_c)} & 0 \\ 0 & \sqrt{(1-\delta_2)^N} \end{pmatrix}, \tag{10}$$

here δ_c is the compensatory dissipation of each compensation optical element. The practical transmissivity $(1-\delta_2)^N$ and the inherent dissipation δ_1 were measured to be 88% and 4%, respectively. W_M introduces the phase difference φ of big MZIs via the HR$_M$, and we adjust

the voltage at *PZT* via computer controlled system to get the instructive interference at D_1, and meanwhile we get the destructive interference at D_2. Then the optimized reliability η_0 can be obtained when we lock the phase difference of two big MZIs to be $\varphi = 2n\pi$.

Figure 6 shows the dependence of reliability η_0 on δ_c for $M = 3$ and $N = 8$, the blue solid line is the theoretical result, the red points show the experimental data η_0 with different δ_c. The measured reliability is $\eta_0 = 12.9 \pm 0.08$ without compensatory dissipation ($\delta_c = 0$) in this scheme. The tendency of improvements with dissipation compensation is obvious, and show agreement with the theoretical predication. The optimal improved value $\eta_0 = 25.1 \pm 0.36$ is obtained. When the bottom path on the big MZI has a definite dissipation ($\delta_1 + \delta_c = 0.355$), the value of the reliability η_0 will be infinity in theory for full communication process, however, in practical setup, the inevitable dissipation from the random variations of optics could not be fully compensated in experiment, as seen in Fig. 6.
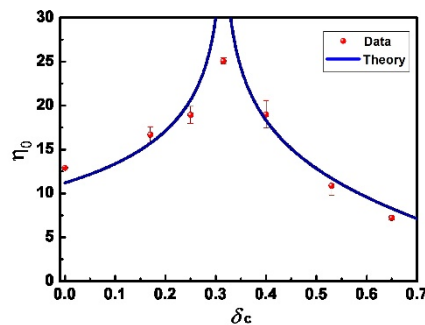

Fig. 6. The improved reliability η_0 vs balanced dissipation δ_c

5. Summary

We have numerically simulated the reliability of the counterfactual deterministic communication which the dissipation must be considered in an actual system. It comes to the conclusion that the inevitable loss or dissipation limits the number of MZIs and beam splitters, showing in principal that the communication scheme could be carried out with a finite number of imperfect interferometers, and the reliability can be improved with dissipation compensation. The transfer-matrix method is also applied in this system which has been used to discuss the reliability of information transmission. We have greatly improved the reliability of the protocol in experiment and proved the feasibility of our design concept.

Funding